infrastructures

MDPI

Article

Crowd–Structure Interaction on Building Floors for Event Use—An Experimental Study

Vincent Baumann [1,*], Lucas Adélaïde [2] and Pierre Argoul [2,3]

[1] Structural Engineering Department, Setec Bâtiment, 42-52 quai de la Rapée, 75012 Paris, France
[2] EMGCU Laboratory, Materials and Structures Department, Université Gustave Eiffel Cité Descartes, Bâtiment Bienvenüe 14-20 Boulevard Newton, 77420 Champs-sur-Marne, France; lucas.adelaide@univ-eiffel.fr (L.A.); pierre.argoul@univ-eiffel.fr (P.A.)
[3] LVMT Laboratory, Ecole Nationale des Ponts et Chaussées & Université Gustave Eiffel, 6-8 Av. Blaise Pascal, 77420 Champs-sur-Marne, France
* Correspondence: vincentbaumann@hotmail.fr; Tel.: +33-6-33-90-37-65

Abstract

This paper investigates crowd–structure interaction (CSI) on low-frequency floors during concert events. The findings are based on a full-scale experimental study conducted on a floor prototype designed for a specific infrastructure project. Both the structure and the participants were instrumented while performing various rhythmic activities, such as bouncing and jumping. The study emphasizes the necessity of defining load cases based on the music signal, as its frequency and amplitude may have a variable probability of occurrence. Furthermore, human sensitivity to floor vibrations is examined, with specific comfort thresholds identified for different activities. The core contribution of this work lies in quantifying coordination levels for groups of up to 97 jumping individuals, extending the limited existing literature and refining the definition of jumping crowd actions. Additionally, modal characterization of the unoccupied prototype was performed to evaluate the equivalent damping provided by individuals during standing, walking, bouncing, or jumping. The results demonstrate that while the crowd has a significant impact on the system's equivalent damping, this effect remains highly variable. Finally, the implications of these findings for structural engineering and design practices are discussed.

Keywords: floors structural dynamics; concert; crowd motion; damping; crowd–structure interaction; full scale testing

Academic Editors: Alessio Cascardi and Joan Ramon Casas Rius

Received: 24 December 2025
Revised: 3 March 2026
Accepted: 24 March 2026
Published: 1 April 2026

1. Introduction

Accurate modeling of dynamic crowd loading is a critical challenge for buildings featuring slender, low-frequency floors. Building on expertise developed since the 1990s for grandstands and concert halls, structural research has increasingly focused on the complex phenomenon of Crowd–Structure Interaction (CSI).

Recent incidents, such as the collapse of a grandstand at the Nijmegen stadium in 2021 and the disturbing resonance observed in a Detroit concert hall in 2022, demonstrate the urgent need to extend CSI studies to general-purpose buildings. Such structures often undergo significant changes in usage or require a high degree of versatility to accommodate a variety of events. The present study is based on the design of a contemporary art center [1], which features large-span floors intended for events with a high occupancy such as fashion shows and concerts.

Currently, structural engineers have few guidelines for such specific load cases. While foundational approaches were provided by British codes [2–5] and German experts [6,7], further experimental validation remains essential. Additional recommendations can be found in Canadian [8], American [9,10], European [11–13], and international guides [14].

The literature review is initially focused on these standards to highlight the gap between current design practice and experimental reality. Of course, research is pushed forward on initial topics such as stadia [15,16] or footbridges [17], but also on stochastic analysis methods [18], acquisition systems in line with technological developments [19], and individuals' responses to stimuli [20]. This paper should emphasize the relevance of current research topics in order to continue to develop more refined or sophisticated approaches.

For an individual in motion, the induced excitation is typically modelled as a periodic force to simplify the analysis [21,22], which can be decomposed into a Fourier series. This allows the overall vertical action of the crowd to be determined, provided that parameters such as spatial distribution and individual action variability are correctly accounted for. Beyond the ability to simply synchronize with a rhythmic source, it is crucial to characterize the degree of coordination between individuals and their ability to maintain this coordination over time [23,24].

Once the loading is defined, the mechanical interaction between the crowd and the floor must be accurately described. The structural response can, in turn, alter human behavior [25]; depending on the vibration levels, individuals may adjust their action in terms of amplitude, frequency, or phase. Conversely, the modal parameters of the coupled system, particularly the damping ratio, can be significantly modified by the presence of a crowd, whether active or static. These effects are of paramount importance for the safety and serviceability of low-frequency floors [26,27].

To broaden the available experimental database, a full-scale prototype inspired by the reference project [1] was constructed, featuring a design similar to that of a steel–concrete composite bridge. An initial test campaign was conducted to identify the structure's modal characteristics and to analyze the nonlinear evolution of damping in relation to vibration amplitude. The floor was further evaluated using removable viscous dampers. Progressive tests were then performed with groups of active participants ranging from 12 to 108 individuals, in order to establish a robust correlation between dynamic loading and structural response.

Through this research, we identified critical parameters, such as auditory cues (music) and structural vibrations, that significantly influence crowd behavior. The primary contribution of this work lies in the empirical evaluation of coordination levels within a jumping crowd. By extending the existing experimental data to groups of approximately 100 individuals, this study provides a substantial expansion of the current literature and experimental charts. Furthermore, by establishing the modal properties of the unoccupied structure across varying vibration amplitudes, we quantify the added damping effect of the crowd based on the specific type of activity. While these results are derived from a simplified interaction model, they provide a sufficiently representative framework for structural analysis.

The remainder of this article is organized as follows:

Section 2 details the experimental protocol, covering the design and construction of the prototype, the instrumentation deployed for both the structure and the participants, and a description of the three testing phases along with an overview of the initial raw data.

Section 3 categorizes the findings into two main thematic groups. The first focuses on analyzing the influence of music, the impact of floor vibrations on human behavior, and the evolution of jumping coordination as a function of group size. The second group addresses damping characterization, distinguishing between the intrinsic structural damping and the damping induced by a static or active crowd (walking, bouncing, or jumping).

Section 4 concludes the study by addressing three fundamental questions in floor structure design: impact resistance, resonance management, and fatigue life analysis.

2. Experimental Protocol

2.1. Prototype Design and Construction

The prototype consists of a 48.1 m^2 (18.32 m × 2.626 m) composite floor system comprising 750 mm high steel beams connected to a 120 mm thick Cofrastra 40 composite slab (Figure 1). The floor is supported by two steel frame abutments anchored to the laboratory test slab. Prefabricated concrete slabs are placed on top of the prototype to provide additional mass without contributing to the global stiffness of the structural system, due to the presence of hollow joints spaced at 1.5 m intervals. This arrangement ensures a participating mass representative of the reference project (ceiling, building services, equipment, floor finishes…). Removable V-shaped dampers are installed at mid-span and supported by a transverse beam located at the base.

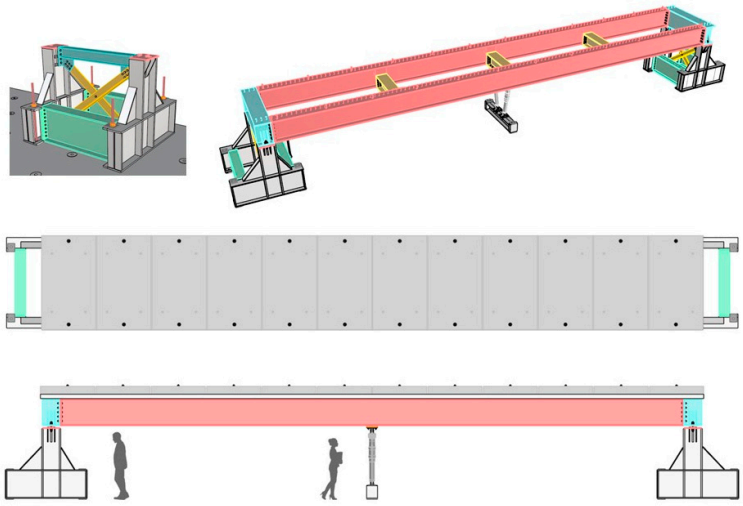

Figure 1. General design of the prototype.

The steel floor structure comprises two welded longitudinal I-beams (denoted PL in red, section dimensions: H = 750 mm, B = 400 mm, tw = 12 mm, tf = 30 mm) spaced by I-beams (denoted T in yellow; H = 500 mm, B = 400 mm, tw = 20 mm, tf = 40 mm) and connected to the C-shaped transverse edge beams (PRT: blue; section H = 750 mm, B = 500 mm, tw = 40 mm, tf = 30 mm), to which the steel support points are welded.

The floor of the prototype rests on steel bearings at the top of the abutment, 17.72 m apart in the longitudinal direction and 2.226 m apart in the transverse direction. Lateral steel cleats restrain the supports in the transverse and longitudinal directions. The support conditions are defined as follows: the south-west support is fixed; the north-west support is restrained in the longitudinal direction only; the south-east support is restrained in the transverse direction only; and the north-east support is free.

The prototype was installed on the laboratory test slab, which ranges in thickness from 90 cm to 125 cm and is supported by a 3 m × 3 m waffle-type substructure (Figures 2 and 3). It is surrounded on all sides by 1.5 m wide self-supporting scaffolding (Figure 4), with two staircases located at the south-west and north-east corners. A clearance gap of approximately 6 cm (with a minimum of 2 cm at the connection brackets) is maintained between the scaffolding and the deck to prevent any contact during testing. The scaffolding serves as a guardrail during deck testing, as a working platform for instrumentation management, and as a waiting area throughout the tests.

Figure 2. Long span floor prototype: Intrados.

Figure 3. Removable pair of viscous dampers.

Figure 4. Long span floor prototype: Extrados.

2.2. Sensors

The prototype is equipped with the following sensors (Figure 5):

- Six LORD wireless accelerometers with independent acquisition (green markers)
  - Sampling frequency: 512 Hz;
- Two LVDT displacement sensors on CATMAN control unit (red markers)
  - Limit stroke of 50 mm with an initial rod retraction of 15 mm;
- Two Velocimeters on CATMAN control unit (blue markers);
- Three temperature sensors on CATMAN control unit for dampers (purple markers);

- Two optical fibers connected to an independent acquisition unit (blue lines) to validate modal identification performed with accelerometers and investigate a complementary and innovative approach [1].

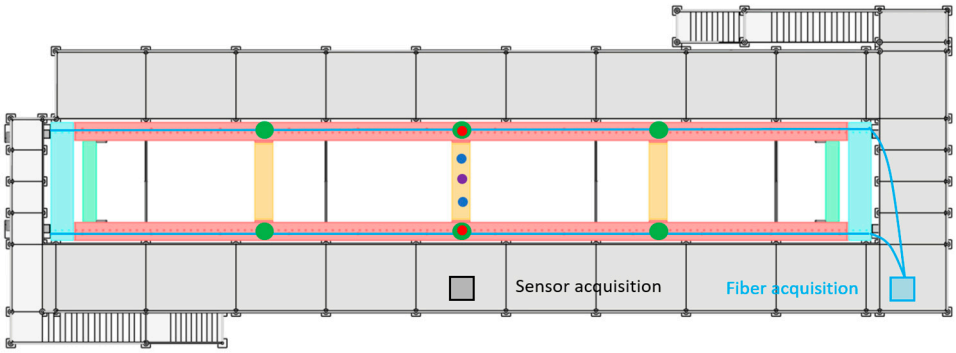

Figure 5. Types and location of sensors of the prototype.

Group and crowd dynamic loading was generated by architecture students from the École Nationale Supérieure d'Architecture de Paris Val de Seine, all of whom provided informed consent prior to participation. Two types of systems were used to experimentally measure individual actions. First, twelve pairs of Kinvent K-Force force plates were deployed (Figure 6a). The number of plates was limited for economic reasons; however, this configuration ensured at least one pair per paving slab for each designated leader during crowd tests, or sufficient instrumentation to monitor a group of twelve participants centered on the prototype. In addition, a COMETA WaveTrack_4 acquisition system equipped with twelve inertial measurement units (IMUs) was used as an indirect measurement system to compare with the force plate results. For each test, ten sensors were assigned to ten active participants (Figure 6b). The method consists of measuring the vertical acceleration at the level of the seventh cervical vertebra (C7), as proposed by McDonald and Živanović [28], and multiplying it by the participant's mass to estimate the applied force. The two remaining COMETA sensors were used to synchronize the overall acquisition system. They were attached with adhesive adjacent to the central LORD accelerometers on the underside of the steel beams. Finally, four GoPro HERO10 cameras were used to record the tests.

(**a**) (**b**)

Figure 6. (**a**) Kinvent K-Force force plates and (**b**) COMETA accelerometers.

2.3. Experimental Protocol and Rough Results

2.3.1. Phase 1: Modal Characterization of the Prototype with and Without Dampers

The modal characterization of the prototype was performed using a 320 kg shaker from ULiège (Figure 7), considering configurations with and without additional slabs, and

with and without dampers. A complementary test was conducted to investigate the modal properties of the prototype with forty participants uniformly distributed over the floor, without dampers.

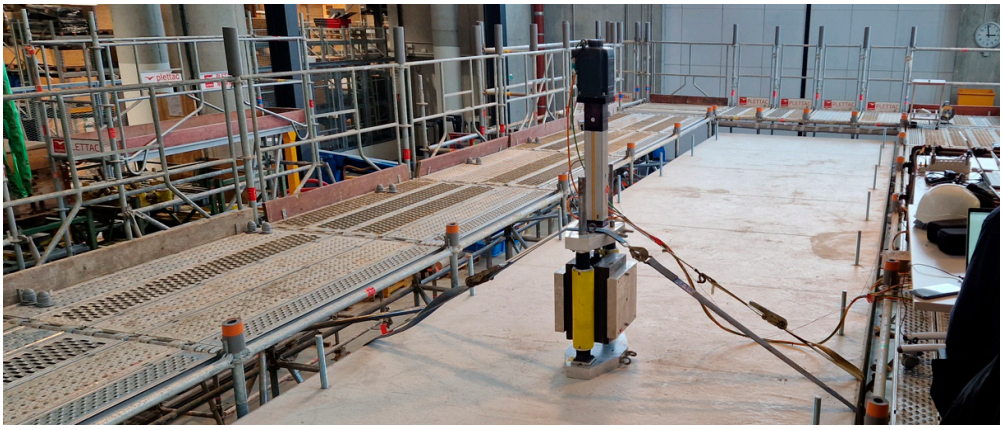

Figure 7. Tests with ULiège mechanical shaker on 10 March 2023.

Vibrations on the shaker are acquired using PCB accelerometers measuring in the range of ±2 g with a sensitivity of 1000 mV/g. The sampling frequency is set at 2048 Hz (Shannon frequency of 1024 Hz), which largely covers the frequencies of the study. Decimation at a frequency of 64 Hz is performed for analysis. Excitation was performed in broadband using white noise selected to excite a wide frequency range (0.1–10 Hz). In all tests performed, frequency scanning in steps was repeated for different levels of acceleration at the shaker (23 mg, 92 mg, 250 mg, 394 mg, and 600 mg).

2.3.2. Phase 2: Tests with Fully Instrumented Active Groups: Training and Calibration

These group tests were conducted to assess the participants' ability to drive the prototype into resonance through activities such as bobbing (knee bending while maintaining continuous contact with the floor) or jumping. By limiting the number of active participants to ten, the execution of the tests could be better controlled, while ensuring that all participants were instrumented to establish a precise relationship between the excitation and the structural response. A detailed description of this phase is provided in reference [1].

2.3.3. Phase 3: Crowd Testing: Bobbing and Jumping Tests with Music and Metronome with and Without Dampers

The tests were conducted over two full days and one half-day, on 16 March, 13 April, and 20 April 2023, respectively (Figure 8). The test campaign was organized to maintain a consistent level of participant motivation. Accordingly, the sessions were scheduled at least one week apart, as reduced motivation could have influenced the experimental results.

Several types of tests were conducted over the three test days:

- Bobbing tests with metronome (Tests A with 102 participants);
- Jumping tests with metronome (Tests E with 96 to 97 participants);
- Free dance with music (Tests F with 102 to 108 participants);
- Metronome Jumping tests with dampers (Tests G with 12 to 97 participants);
- Metronome Jumping tests without dampers (Tests H with 12 to 95 participants).

Figure 9 presents the maximum accelerations recorded during the three main crowd test series. For clarity, series A, E, and F were performed with dampers installed. The metronome-paced jumping tests (Series E) exhibit a pronounced acceleration peak at a pacing frequency of approximately 2.7 Hz. This value is close to half the fundamental natural frequency of the structure (f_r around 5.4 Hz, see Figure 9), as identified from shaker

tests. In Figure 9, $f_{r,h=2}$ denotes the excitation frequency capable of triggering resonance for the considered harmonic order h. These results indicate that crowd jumping does not significantly alter the fundamental frequency of the unloaded prototype equipped with dampers. In contrast, the metronome-paced bobbing tests (Series A) display two acceleration peaks around 2.2 Hz and 2.4 Hz. This suggests a downward shift in the apparent natural frequency ranging from approximately −20% to −10%, which can be attributed to the contribution of the crowd to the modal mass when participants remain in continuous contact with the structure. The free-dancing tests with music (Series F) appear intermediate between Series E and A. Multiple acceleration peaks are observed, indicating variability in the fundamental frequency of the coupled crowd–structure system, depending on whether participants predominantly jump or bob in mixed excitation scenarios.

Figure 8. Free dance with music (Example of at test F).

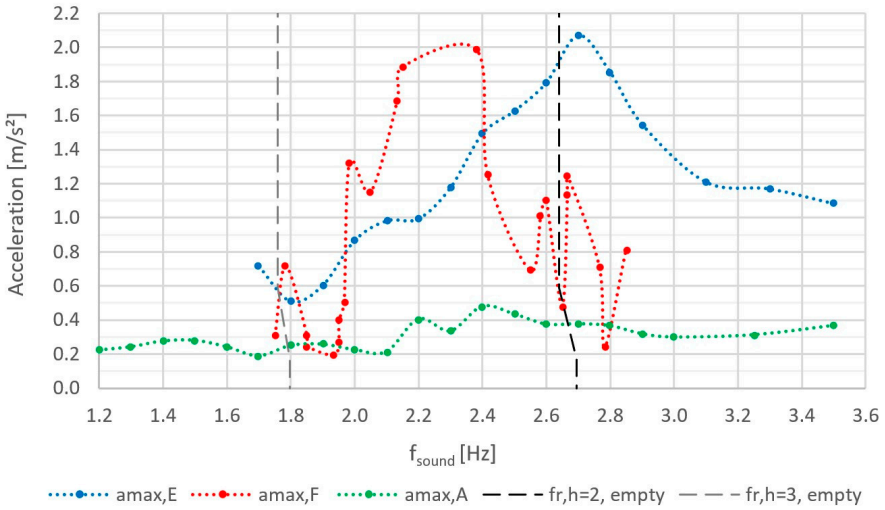

Figure 9. Maximum peak accelerations of series E, F and A as a function of tempo.

Figure 10 presents the impact factors for the three series A, E and F. The maximal individual impact factor $k_{p,max,i}$ is defined as the ratio between the maximum force F_i generated by participant i and the corresponding body weight G_i:

$$k_{p,max,i} = \frac{\max(F_i(t))}{G_i}. \quad (1)$$

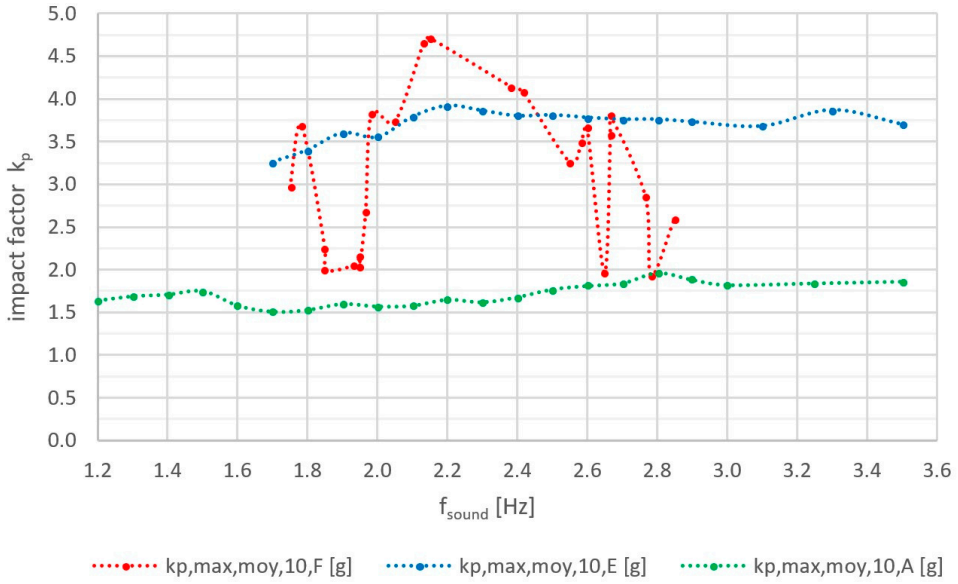

Figure 10. Impact factor of test series E, F and A as a function of tempo [Hz].

The indicator $k_{p,max,moy,10}$ corresponds to the average action of the ten uniformly distributed leaders, considered representative of the loading applied by the members of their respective groups on each paving slab:

$$k_{p,max,moy,10} = \frac{\sum_{i=2}^{11} k_{p,max,i}}{10}. \quad (2)$$

Video analysis was used to validate the extrapolation of the interpretation established from the leaders (one leader representing nine participants on each paving slab, excluding the edge slabs).

For the bobbing test series (A), the load remains relatively constant across the tested pacing frequencies. In contrast, for the jumping test series (E), a higher overall impact factor is observed around 2.2 Hz. This may reflect the greater ease with which synchronized jumping can be performed near this frequency. The impact factors recorded during the free-dancing tests (Series F) exhibit significantly greater variability. This variability likely reflects differences in participants' responses to the music, leading to less consistent excitation patterns.

Figure 11 presents the maximum accelerations recorded at mid-span of the prototype as a function of the increasing number of participants during metronome-paced jumping tests conducted with dampers installed. A clear reduction in coordination effects can be observed as the group size increases. The maximum acceleration does not increase proportionally with the number of participants, highlighting the influence of loss of synchronization within larger groups. A pronounced acceleration peak remains visible around 2.6–2.7 Hz, consistent with resonance associated with the second harmonic. For reference, Annex C of ISO 10137 [14] indicates a peak acceleration limit of approximately 1.41 m/s^2 corresponding to discomfort and 2.83 m/s^2 corresponding to panic conditions for stadiums and assembly floors [1]. By cross-referencing data from SCI P354 [5], NBC [8], and Bachmann [7], an average discomfort threshold of approximately 1.4 m/s^2 and an assumed panic threshold of approximately 3 m/s^2 may be considered representative values. It should be noted that vibration comfort criteria are frequency dependent [5].

Figure 12 presents the maximum accelerations recorded at mid-span of the prototype as the number of participants increases during metronome-paced jumping tests conducted without dampers. The evolution of the acceleration is noticeably more irregular than in the damped configuration. Away from resonance, a clear increase in peak acceleration with

the number of participants is observed. In contrast, near resonance, higher acceleration levels may be reached with a smaller number of participants. The apparent scatter of the results in the resonance region can be attributed to the strong interaction between floor motion and human movement. The specific investigation of this crowd–structure interaction phenomenon is relatively recent [25] and involves particularly complex issues in terms of physical understanding and modelling.

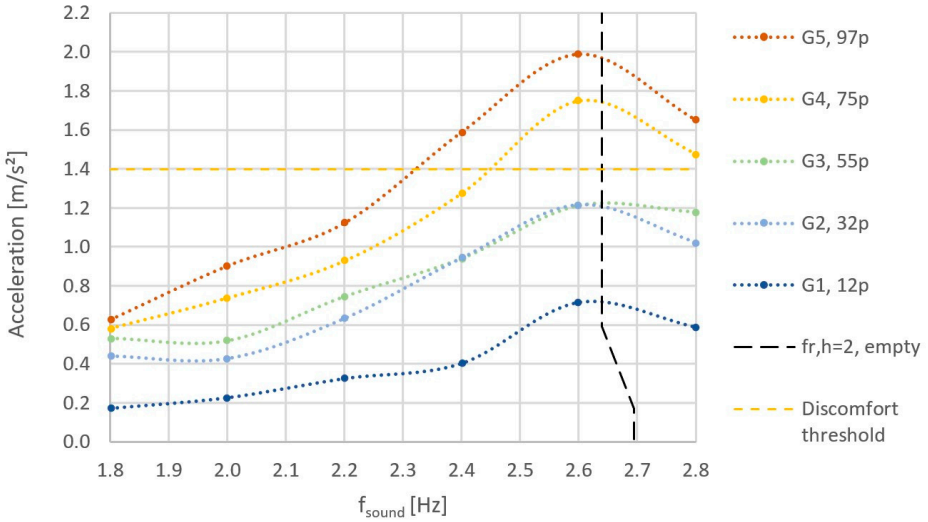

Figure 11. Acceleration for tests G versus the number of people.

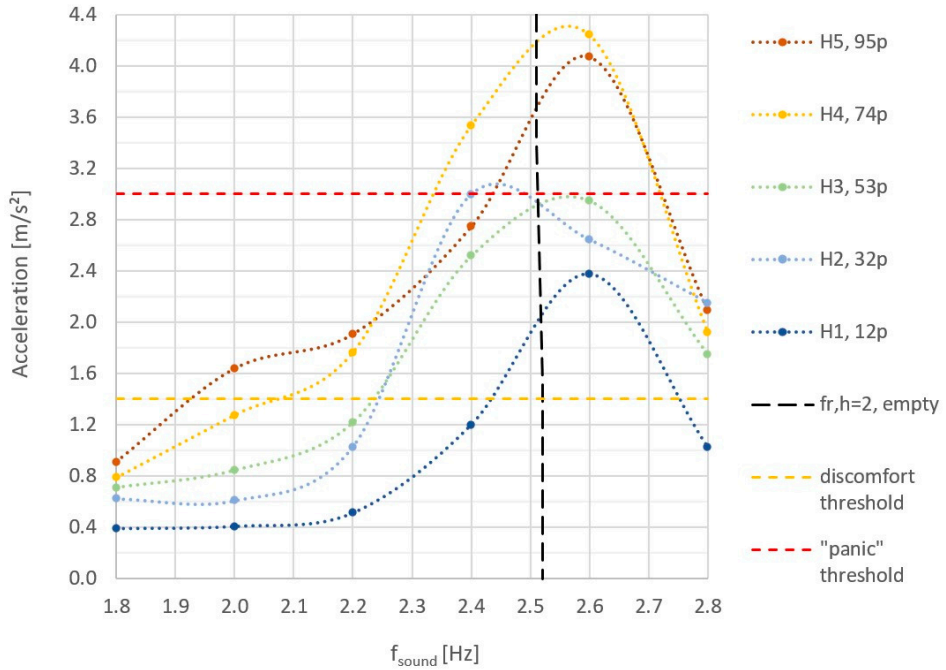

Figure 12. Acceleration for tests H versus the number of people.

3. Results

3.1. Characterization of Crowd–Structure Interaction

3.1.1. Influence of Music on Crowd Action

Coordinated collective action during concerts generally requires the presence of music. Table 1 summarizes the main observable tempo ranges associated with the principal musical genres. These frequency ranges are not intended to be exhaustive, as certain tracks may occasionally fall outside the indicated intervals.

Table 1. Musical genres classified according to usual tempos.

Tempo	Largo Larghetto Adagio			Andante						Moderato						Allegro							Presto						Prestissimo
BPM	60	66	72	78	84	90	96	102	108	114	120	126	132	138	144	150	156	162	168	174	180	186	192	198	204	210			
f [Hz]	1	1.1	1.2	1.3	1.4	1.5	1.6	1.7	1.8	1.9	2	2.1	2.2	2.3	2.4	2.5	2.6	2.7	2.8	2.9	3	3.1	3.2	3.3	3.4	3.5			
Genre	Reggae/Dub																												
				Hip hop																									
				Latino																									
						Rock pop/Folk																							
								Heavy Metal																					
										House																		
											Techno																	
											Electro																	
												Dubstep																
																Drum and bass												
																				Punk Rock								
																				Hardcore/Speedcore (and beyond)								

Tempo distributions by decade were established based on the 100 most popular tracks identified in Spotify decade-based playlists. The overall shape of the distributions remains relatively consistent across decades. A corrected average distribution over the past 60 years was subsequently derived and is proposed as a reference distribution independent of specific eras or musical trends (Corr., Table 2).

Table 2. Distributions by decade, 60 years average and corrected average.

Tempo	Largo Larghetto Adagio			Andante						Moderato						Allegro							Presto						Prestissimo
[BPM]	60	66	72	78	84	90	96	102	108	114	120	126	132	138	144	150	156	162	168	174	180	186	192	198	204	210			
[Hz]	1	1.1	1.2	1.3	1.4	1.5	1.6	1.7	1.8	1.9	2	2.1	2.2	2.3	2.4	2.5	2.6	2.7	2.8	2.9	3	3.1	3.2	3.3	3.4	3.5			
2010s	0	1	1	0	2	5	7	6	1	6	24	33	11	1	1	0	0	0	0	1	0	0	0	0	0	0			
2000s	0	0	1	3	2	3	8	9	6	11	17	13	12	6	2	2	1	1	0	2	0	0	1	0	0	0			
90s	0	0	1	2	1	5	7	11	8	6	16	15	13	6	2	3	1	0	1	2	0	0	0	0	0	0			
80s	0	0	0	1	2	3	5	9	14	13	15	15	7	2	4	2	1	2	1	2	1	0	1	0	0	0			
70s	0	0	2	3	1	1	5	9	9	12	19	13	10	5	1	5	2	2	1	0	0	0	0	0	0	0			
60s	0	0	3	7	5	9	6	7	5	12	10	11	6	5	3	5	3	1	0	1	0	0	1	0	0	0			
Mean	0	0	1	3	2	4	6	9	7	10	17	17	10	4	2	3	1	1	1	1	0	0	1	0	0	0			
Corr.	0.1	0.2	1.3	2.7	2.2	4.3	6.2	8.3	7.1	10.0	16.7	16.7	9.8	4.2	2.2	2.8	1.3	1.0	0.5	1.3	0.2	0.1	0.5	0.1	0.1	0.1			

The reference distribution (Figure 13) exhibits a high density of tracks around 2 Hz (120 BPM), reflecting the strong influence of electronic music. A secondary peak is observed around 1.7 Hz (100 BPM), associated with hip-hop and pop-rock influences. The probability of tracks exceeding 3 Hz (180 BPM) is very low (approximately 1%). Similarly, fewer than 10% of tracks fall below 1.5 Hz (90 BPM).

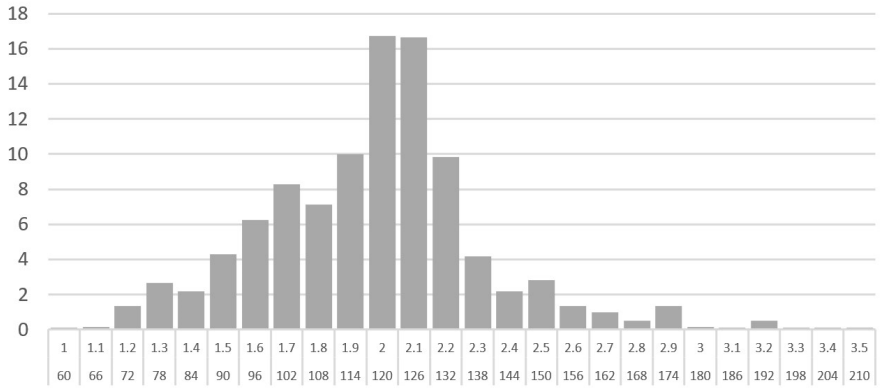

Figure 13. Frequency distribution [Hz–BPM] corrected average over 60 years.

While the statistical distribution of tempos provides a useful basis for assessing the probability of structural excitation at a given frequency, it may in some cases be necessary to

estimate the excitation amplitude associated with a specific music track. The experimental results revealed a progressive reduction in overall loading following each musical "drop". It is therefore possible to estimate the duration of high-intensity crowd excitation by cumulatively accounting for these drops, whose most significant effects typically persist for 10 to 20 s, depending on the case (Figure 14).

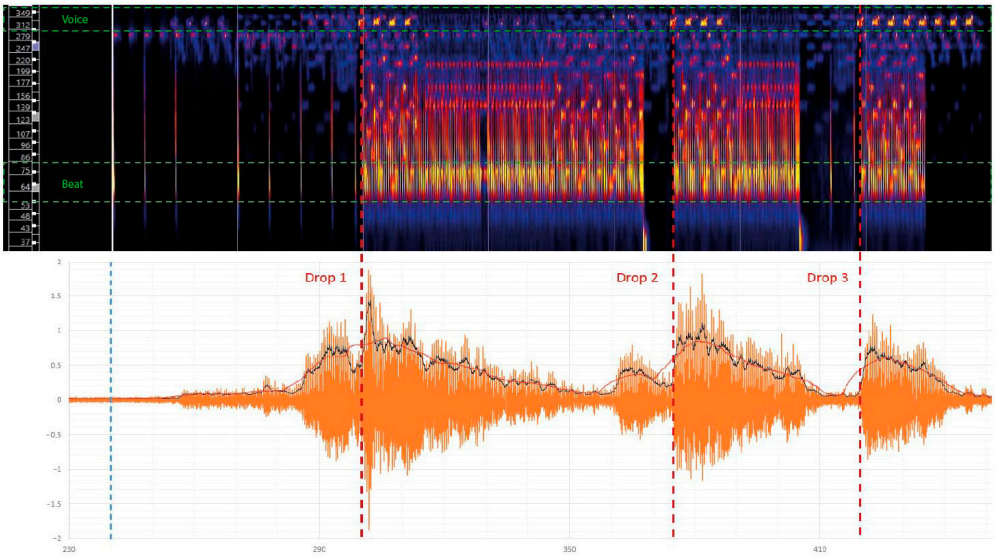

Figure 14. Spectrogram of "Freed from desire" (test F with 102 participants [1]) sound signal in [Hz] and accelerogram [m/s^2] at mid-span.

3.1.2. Influence of Floor's Vibration on Crowd Action

Excluding specific individual cases, the following general observations can be drawn from the experimental survey conducted among participants:

- Sensitivity to vibration varies significantly depending on the activity performed by the individual during testing.
- For stationary participants exposed to floor vibrations, the end-of-comfort threshold is typically observed at approximately 0.5 m/s^2 peak, while the onset of discomfort occurs around 1.5 m/s^2 peak. An adaptation effect was observed between successive vibration test series involving the same stationary individuals, with the end-of-comfort threshold increasing to approximately 1 m/s^2 peak.
- Under concert-like conditions, floor vibration does not appear to influence participant behavior for peak accelerations below 1.4 m/s^2. An end-of-comfort threshold of approximately 1.4 m/s^2 peak may also be considered representative for this configuration.
- The hypothesis of a discomfort threshold potentially leading participants to leave the vibrating floor at approximately 3–4 m/s^2 peak requires further targeted investigation. In such a scenario, a potential beneficial effect could be a reduction in structural response due to unloading, whereas a detrimental effect could involve panic-induced movements.
- In general, participants engaged in bobbing feel less vibration than stationary individuals, and those jumping feel less vibration than those bobbing.
- When all participants are jumping, very high acceleration levels may not be perceived as intolerable or significantly disturbing, whereas such levels would likely be unacceptable for stationary individuals (Figure 15).

Perception differs when participants are free to act, without being guided by a structured experimental framework (e.g., metronome pacing and prescribed movement instructions). This observation reinforces the need to compare the measured responses with real-world conditions—considering contextual factors such as time, location, light-

ing, sound environment, and participant motivation—in order to obtain more reliable assessments of perceived vibration and its impact on motor behavior.

(**a**) (**b**)

Figure 15. During (**a**) and immediately after (**b**) the 16 people jump with a_{pic} = 3.4 m/s^2.

3.1.3. Jumping Coordination of Individuals as a Function of the Size of the Group

For a crowd composed of N individuals with a mean body weight G_{mean}, jumping at an excitation pulsation ω_p, the total force exerted on the structure, $F_{tot}(t)$, may be expressed as a function of the average individual Fourier coefficients α_h, weighted by a coordination coefficient $C_h(N)$ [4]:

$$F_{tot}(t) = N\, G_{mean}\left(1 + \sum_{h=1}^{H} C_h(N)\alpha_h \sin\left(h\omega_p t + \varphi_h\right)\right). \quad (3)$$

The experimental campaign enabled the derivation of curves representing the average and global trends of the weighted Fourier coefficients $C_h(N)\alpha_h$ for up to approximately 100 individuals jumping simultaneously. Figure 16 presents, for each test series (H1 to H5 and G1 to G5), the group Fourier coefficients associated with jumping at excitation frequencies of 2.4 Hz, 2.6 Hz, and 2.8 Hz. This frequency range was selected because it corresponds to the most critical resonance conditions in the present study. In practical applications, structures are generally designed to exhibit a fundamental natural frequency of at least 5 Hz, in accordance with Eurocode recommendations. Under this assumption, resonance may occur at the second harmonic for excitation frequencies around 2.5 Hz, which justifies the selected range. This configuration allows six measurement points to be obtained for a given number N of participants. The average contact ratio for the maximum impact of the 10 leaders over all the tests is 0.37. The average minimum contact ratio of 10 leaders for a single test is 0.32 (i.e., the maximum impact).

For a single individual, the Fourier coefficients were assigned a higher weight (30) in order to define the initial point of the trend curve. The individual action is known for each instrumented individual for all the 30 group tests. The other points, six trials per number N of participants (three tests G and three tests H), were not weighted in the regression analysis. This leads to 60 data points in total per harmonic. Power-law regressions were obtained by linearizing the model through logarithmic transformation and performing least-squares regression in log–log space. Data set are provided in tables in reference [1].

A power-law fit of the form $C_h(N)\alpha_{h,mean} = \mathrm{aN}^{-b}$ is thus performed:

$$\begin{aligned} C_1(N)\alpha_{1,mean} &= 1.73\,\mathrm{N}^{-0.19}\ (R^2 = 0.81,\ 95\%\ CI_a : [1.62,\ 1.85];\ 95\%\ CI_b : [-0.22, -0.17]), \\ C_2(N)\alpha_{2,mean} &= 1.15\,\mathrm{N}^{-0.53}\ (R^2 = 0.94,\ 95\%\ CI_a : [1.05,\ 1.26];\ 95\%\ CI_b : [-0.57, -0.50]), \\ C_3(N)\alpha_{3,mean} &= 0.48\,\mathrm{N}^{-0.72}\ (R^2 = 0.93,\ 95\%\ CI_a : [0.42,\ 0.55];\ 95\%\ CI_b : [-0.77, -0.67]). \end{aligned} \quad (4)$$

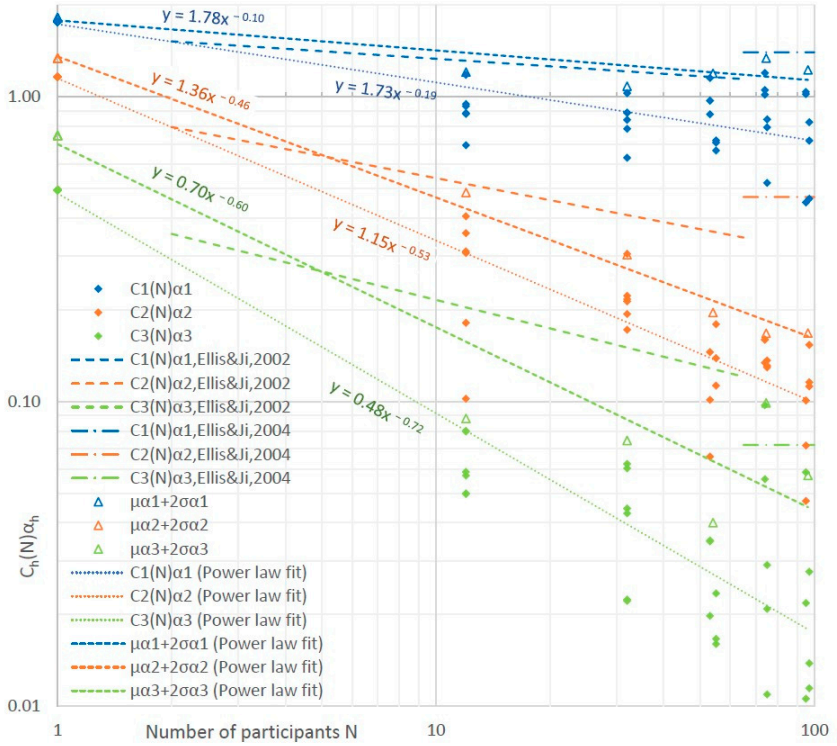

Figure 16. Fourier series coefficients of group $C_h(N)\alpha_h$ [23,24].

To estimate the envelope of extreme test results, the mean value μ_{α_h} of the six measurements for a number N of participants plus two standard deviations σ_{α_h} is also plotted. For a single individual, the Fourier coefficients were assigned a weight of five in order to define the initial point of the trend curve. The resulting envelope equations are given as follows:

$$\begin{aligned} C_1(N)\alpha_{1,95\%} &= 1.78\,\mathrm{N}^{-0.10}\ (R^2 = 0.84,\ 95\%\ CI_a : [1.62,\ 1.97];\ 95\%\ CI_b : [-0.13, -0.06]), \\ C_2(N)\alpha_{2,95\%} &= 1.36\,\mathrm{N}^{-0.46}\ (R^2 = 0.99,\ 95\%\ CI_a : [1.26,\ 1.46];\ 95\%\ CI_b : [-0.49, -0.43]), \\ C_3(N)\alpha_{3,95\%} &= 0.70\,\mathrm{N}^{-0.60}\ (R^2 = 0.93,\ 95\%\ CI_a : [0.48,\ 1.02];\ 95\%\ CI_b : [-0.74, -0.46]). \end{aligned} \quad (5)$$

It can be observed that the envelope curve obtained for the first harmonic is in good agreement with the experimental trend reported by Ellis and Ji [23], as shown in Figure 16. In contrast, the envelope curves derived in the present study for the second and third harmonics exhibit a steeper decay than the corresponding experimental trend curves reported by Ellis and Ji [23]. Overall, the experimental curves proposed by Ellis and Ji appear to align more closely with an upper-bound (envelope) representation than with the mean trend observed in the present experimental results.

Based on the Fourier series coefficients obtained numerically by Ellis and Ji [24], the coefficients proposed for a large number of people (triplet: 1.40/0.469/0.072) already appear to be envelopes of the experimental results for 100 people. In particular, a factor of approximately 2.8 is observed between the value of the second harmonic estimated numerically for a large group by Ellis and Ji [24] i.e., $C_2(N > 400)\alpha_2 = 0.469$ and the maximum experimental value i.e., $C_2(N = 100)\alpha_{2,95\%} = 0.168$.

In summary, the present experimental study extends the reference experimental investigation reported in [23], which was limited to 64 participants, by providing results for group sizes of up to 97 participants. The findings suggest that the experimental coordination factors proposed by Ellis and Ji for the second and third harmonics may be overestimated. Furthermore, the numerically derived coordination factor for the second harmonic for very large crowds ($N > 400$) reported in [24] is likely to be significantly over-

estimated, as coordination does not appear to improve with increasing group size under otherwise identical conditions. It should be emphasized, however, that the present results are based on a specific population of students performing metronome-paced activities. Additional experimental investigations conducted under different conditions are required to confirm, refine, or broaden these conclusions.

3.2. Characterization of Damping

3.2.1. Damping Ratio of the Structure

Returning to the shaker tests, Figure 17 illustrates the variation of the fundamental natural frequency measured with and without the paving slabs. A decrease in natural frequency is observed as the vibration amplitude increases. As these tests were conducted during the initial loading of the structure, this reduction may be attributed to structural settling effects and the initiation of cracking. For a more detailed analysis, the reader is referred to reference [1].

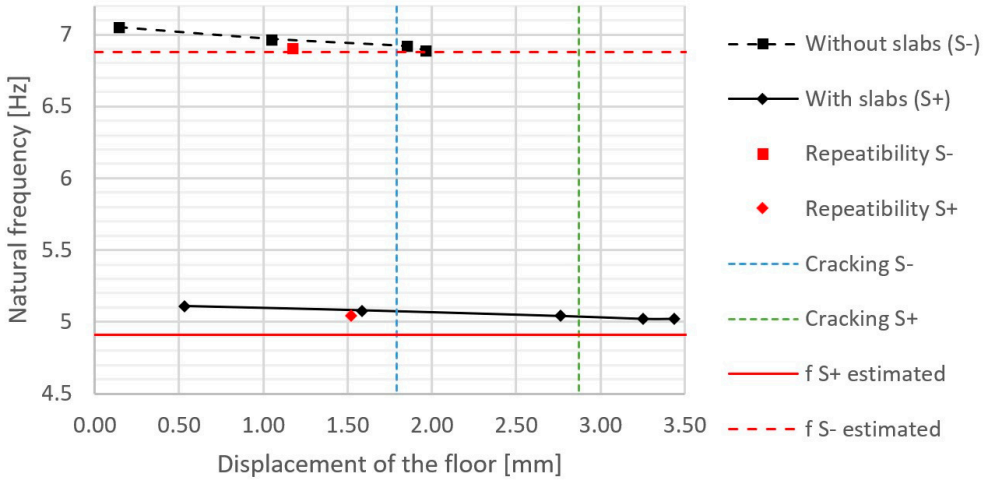

Figure 17. Evolution of natural frequency versus floor displacement without dampers.

Tests conducted on the prototype without dampers showed that the damping ratio increases with vibration amplitude (Figure 18). This increase is nonlinear and becomes more pronounced once the cracking threshold of the concrete slab is exceeded. The presence of the paving slabs induces a compressive prestress in the composite slab, which likely delays the onset of cracking and consequently postpones the marked increase in damping compared with the configuration without paving slabs. While the conventionally measured damping ratio at low amplitude can increase by up to a factor of three at higher amplitudes, the maximum value observed (approximately 1%) remains below the damping levels commonly reported in the literature [12].

An increase in the apparent fundamental natural frequency is observed when the dampers are connected at mid-span to the underside of the prototype (blue curve in Figure 19). This behavior suggests that the damper does not act as a purely viscous device. Instead, it operates in series with a support that is not infinitely rigid, leading to a modification of the effective stiffness of the system.

Shaker tests were conducted to characterize the damping behavior of the prototype equipped with viscous dampers. These tests allowed the identification of an activation threshold of approximately 0.35 mm, as well as an unexpected maximum damping level compared with the value anticipated from the manufacturer's factory tests (Figure 20). The flexibility of the support likely reduces the effective efficiency of the damper. Nevertheless, the equivalent damping ratio remains significantly higher when paving slabs are present,

reaching approximately 6% at low vibration amplitudes, compared with about 0.3% for the undamped configuration.

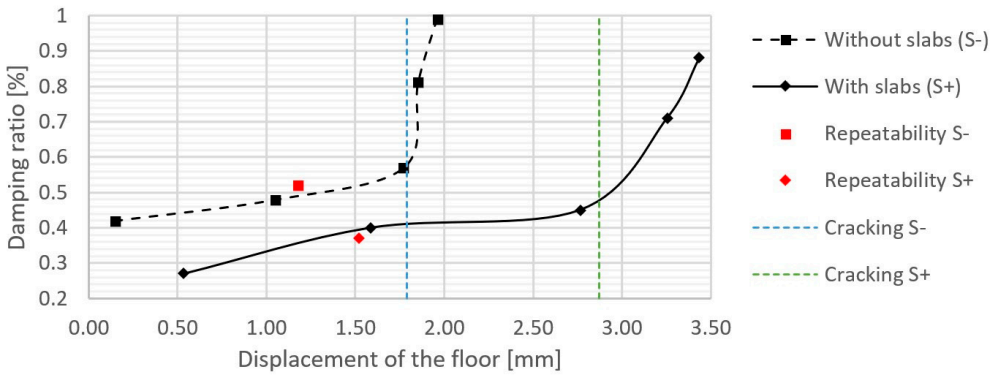

Figure 18. Evolution of damping versus floor displacement without dampers.

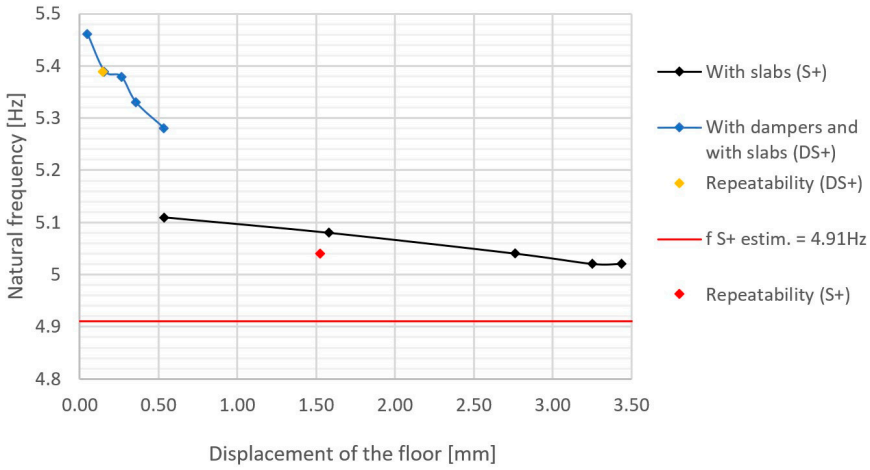

Figure 19. Evolution of frequency with paving slabs versus floor displacement.

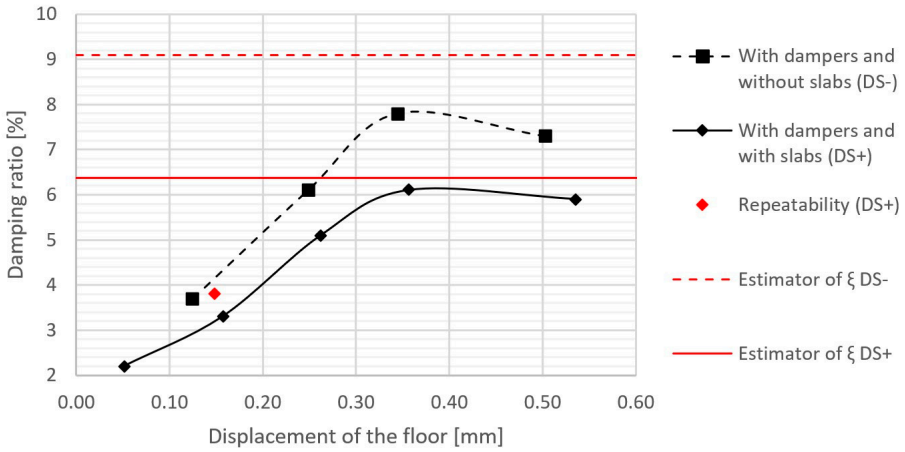

Figure 20. Variation in damping with dampers with and without slabs versus floor displacement.

3.2.2. Equivalent Damping of a Static Crowd

In the case of a concert hall floor, it is relevant to consider a generalized excitation configuration that more closely reflects actual usage conditions. A two-degree-of-freedom (2-DOF) approach is proposed; however, the excitation is formulated as classical dynamic loading applied directly to the structural system (Figure 21). This framework enables a two-step analysis:

- Step 1: Determine the equivalent intrinsic damping of the crowd–structure system.
- Step 2: Perform a dynamic analysis of an equivalent single-degree-of-freedom (SDOF) system using the damping ratio identified in Step 1.

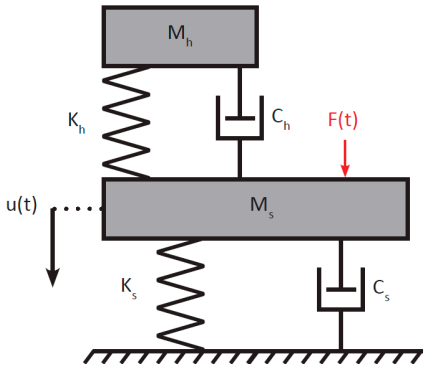

Figure 21. Modelling variant with two degrees of freedom for the crowd–structure system.

This model can be more or less sophisticated in the literature [29–32], and we choose here to test a simple one. The objective is therefore to be able to use the analytical expressions for so-called Tuned Mass Dampers (which is not the case here, or purely by pure coincidence) to estimate the equivalent damping through the evaluation of the maximum dynamic amplification factor.

The dynamic amplification factor of the two-degree-of-freedom system, which is based on non-zero structural damping ξ_s and harmonic excitation pulsation ω, can be determined using the following expression, which is taken from the thesis work of A. Allani [33], and which uses dimensionless parameters:

$$A(\beta) = \frac{\sqrt{(\alpha^2 - \beta^2)^2 + (2\xi_h\beta\alpha)^2}}{\sqrt{[(\beta^2 - \alpha^2)(1 - \beta^2) + \mu\beta^2\alpha^2 + 4\alpha\xi_s\xi_h\beta^2]^2 + [2\xi_h\alpha\beta(\beta^2 + \mu\beta^2 - 1) + 2\xi_s\beta(\beta^2 - \alpha^2)]^2}}, \quad (6)$$

$$A(\beta) = \frac{u_{dyn}}{u_{stat}},\ \alpha = \frac{\omega_h}{\omega_s}, \beta = \frac{\omega}{\omega_s}, \mu = \frac{M_h}{M_s}. \quad (7)$$

It should be noted that for $\xi_s = 0$, Den Hartog's classical solution is recovered, as recalled in the SETRA guide [12]. The approximate equivalent damping of the coupled system reduced to a one-degree-of-freedom oscillator with pulsation $\omega_{eq} = \omega_s\ \beta_{A_{MAX}}$ and mass $M_{eq} = M_h + M_s$ is determined by the following formula:

$$\xi_{eq} = \frac{1}{2\ max(A(\beta))}. \quad (8)$$

The validity of the previously proposed mistuned damper modelling approach is assessed using the test configuration involving 40 stationary participants, which results are given for a shaker test at 250 mg in Table 3.

Table 3. Modal properties measured with slabs and 40 static individuals.

FRF	a_{max} [m/s^2]	Damping Ratio [%]	Frequency [Hz]	Modal Masses [t]
03_250 mg	0.441	3.26	4.91	27.0

An acceleration close to 0.5 m/s^2 was obtained, which also makes it possible to recall the modal properties obtained in a no-load condition with slabs for this level of acceleration in Table 4. It represents a standard comfort acceleration limit in structural vibration serviceability. Moreover, since damping in such structure is amplitude-dependent,

it was necessary to maintain a consistent order of magnitude for the support acceleration across various loading configurations. This consistency allows for a valid comparison of results with and without participants, ensuring that observed changes in damping ratios can be attributed to the crowd–structure interaction. A natural frequency of 5.04 Hz is adopted in the subsequent analysis (compared with 5.11 Hz measured during the tests) to take into account the damage caused by the tests carried out in the meantime.

Table 4. Modal properties measured with slabs and without people.

FRF	a_{max} [m/s^2]	Damping Ratio [%]	Frequency [Hz]	Modal Masses [t]
01_23 mg	0.551	0.27	5.11	26.6

The relevant modal properties of the unloaded support structure are provided in Table 5.

Table 5. Properties of the structure.

Total mass of the structure	$M_{tot,s}$ [kg]	55,454
Generalized mass of the structure	M_s [kg]	25,730
Damping ratio	ξ_s	0.27%
Damping	C_s [kg/s]	4400
Natural frequency of the structure	f_s [Hz]	5.04
Natural pulse of the structure	ω_s [rad/s]	32

The next step is to physically characterize the crowd as a mistuned damper in Table 6 as reported in the literature. Average modal characteristics are adopted for each participant, namely a damping ratio of 22% [31] and an assumed natural frequency of 5.67 Hz.

Table 6. Participant group properties.

Average mass of a person	m_h [kg]	66.4
Decking area	S [m^2]	48
Number of static people on the structure	N	40
Density of static people on the structure	d [p/m^2]	0.8
Total mass of people	$M_{tot,h}$ [kg]	2656
Generalized mass of people	M_h [kg]	1480
Damping ratio	ξ_h	22%
Damping	C_h [kg/s]	23,212
Natural frequency of a person	f_h [Hz]	5.67
People's own pulse	ω_h [rad/s]	36

Figure 22 shows the dynamic amplification factors for three configurations:

- Without public (M_h = 0, classic single-degree-of-freedom oscillator formulation);
- With the public but without the structure's own damping (ξ_s = 0, Den Hartog's solution);
- With the public and non-zero structural damping

An overall experimental damping ratio of 3.26% is obtained when assuming a human damping ratio of 22% [31] and a natural frequency of 5.67 Hz for each participant. However, these individual parameters are likely to vary slightly in practice, depending on the morphology and posture. It is therefore relevant to examine the evolution of the damping

ratio as a function of the natural frequency of the human oscillator, sweeping between 2.3 Hz and 6 Hz and setting the damping parameter accordingly. Figure 23 shows that a reduction in the natural frequency of people has a theoretically non-negligible influence. If people become more flexible, the natural frequency decreases and leads to an increase in equivalent damping until the threshold of 4.7 Hz is reached. At this point, the damping ratio will decrease.

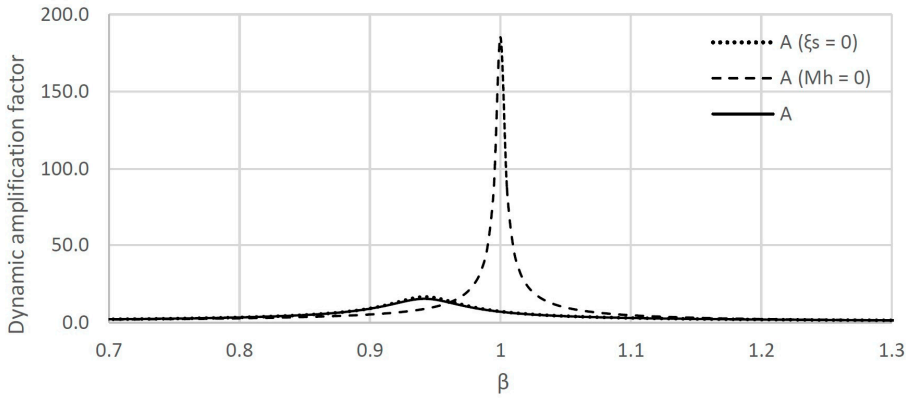

Figure 22. Dynamic amplification according to public presence and structural damping.

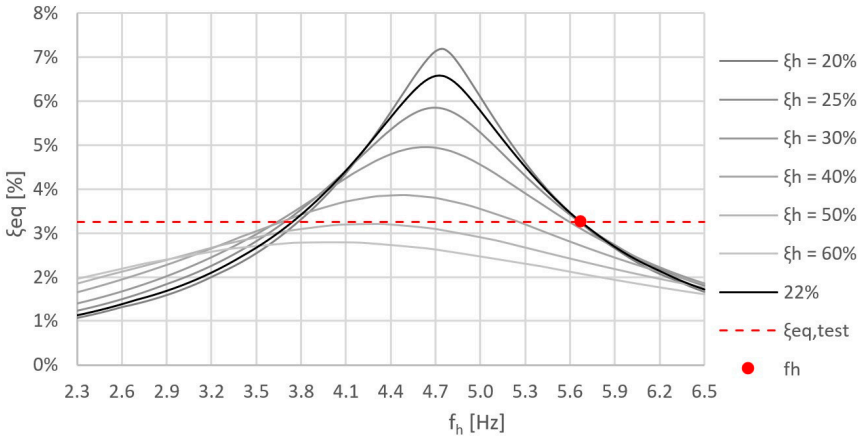

Figure 23. Abacus of individual parameters for tests with 40 static people.

3.2.3. Equivalent Damping of an Active Crowd (Walking, Bobbing or Jumping)

The mistuned mass damper modelling approach yields predictions that are in good agreement with the experimental results.

In practice, the results indicate that individuals contribute significantly to the overall damping of the composite structure, which exhibits very low intrinsic damping in the unloaded configuration. For structures expected to host crowds in continuous contact with the floor, neglecting this additional damping contribution may lead to overly conservative predictions of vibration response, at least with regard to serviceability criteria related to comfort and fatigue verification. The corresponding observations and quantitative estimates are summarized in Table 7.

Jumping does not provide significant additional damping. This is problematic because it is the most powerful action. For the design of structures intended to host concerts or similar events, it is therefore prudent to verify structural resistance and serviceability without accounting for damping contributions from occupants during synchronized jumping. In addition, experience shows that there is no-panic reaction or cessation of activity in the case of a generalized jumping configuration inducing high accelerations because the participants do not feel them during the activity.

It is difficult to quantify precisely the damping provided by the public because the equivalent damping depends on the natural frequency of individuals, which is linked to their posture and their level of activity. According to the estimates reported in Table 7, a crowd density of two people/m^2 standing on a structure can generate a damping ratio ranging from approximately 3% to 15%, for relatively small—and not easily predictable—variations in individual natural frequency. Such variability may encourage designers to adopt conservative values from the lower bound of this range for design purposes. However, this variability should be interpreted in context: even a damping ratio of 3% remains substantially higher than the intrinsic structural damping ratio of approximately 0.3% measured for the unloaded structure.

Table 7. Variability of damping depending on activity [1].

Activity	Measured (* Estimated)		Estimated Variation Range			
			Min		Max	
	d	ξ_{eq}	f_h	$\xi_{eq,min}$	f_h	$\xi_{eq,max}$
	[p/m^2]	[%]	[Hz]	[%]	[Hz]	[%]
Shaker and 40 static people	0.8	3.26	2.3	1.1	4.8	6.6
Shaker and 18 static people	0.4	1.99	2.3	1.0	4.8	5.3
Shaker and 40 people walking	0.8	2.34	2.3	1.1	4.8	5.0
Dance for 190 people and 714 people * (estimate based on reference floor)	0.8	1.8	2.3	1.8	3.8	4.9
	3.0	3.6	5.0	3.6	3.5	13.9
Bobbing for 10 people + 2 static people	0.3	1.04	2.3	0.8	4.9	3.5
Jump of 10 people + 2 static people	0.3	0.69	2.3	0.5	5.0	1.0
	0.3	0.53	2.3	0.3	5.0	0.8
Stop of 10 people jumping (start and end of the stop phase)	0.3	2.58	2.3	0.8	4.8	3.8
	0.3	1.76				
Stop of 95 people jumping (start and end of the stop phase)	2.0	7.45	6.5	2.9	4.2	15.5
	2.0	4.32				

4. Discussion

These experiments aim to address three key questions relevant to structural design:

- Impact: Is a concert involving generalized synchronized jumping likely to produce local dynamic loads exceeding the static load-bearing capacity of the floor system?
- Resonance: Can structural resonance induced by generalized jumping generate elastic dynamic response forces exceeding the global static resistance of the structure?
- Fatigue: Is a steel structure susceptible to fatigue damage after repeated concert events, even if its static resistance is sufficient to accommodate resonance effects induced by jumping?

4.1. Impact

Impact Standard short-span floor systems are typically designed for imposed loads below 500 daN/m^2 [11]. However, three 70 kg individuals per square meter jumping in synchronization may generate dynamic loads of about 1000 daN/m^2 (see Section 3.1.3). This may explain local failures observed on decks spanning between closely spaced beams or on suspended floors.

4.2. Resonance

Resonance affects the global response of low-frequency floors, typically spanning several dozen square meters. In such cases, the number of occupants may reach several dozen or even several hundred. Experimental tests with one hundred students jumping in synchronization show that the coordinated second-harmonic Fourier coefficients (Figure 16) are nearly three times lower than the numerical values proposed in BRE Digest 426 [4]. Since direct resonance is generally avoided in design, the second harmonic becomes the governing issue for low-frequency floors, whose natural frequency may be around 5 Hz for concert venues, as permitted by French regulations [34].

However, even if the observed coordination is lower than that proposed in BRE Digest 426 [4], resonance predicted using the present experimental coefficients may still govern the design of floors with very low damping. Two design strategies may therefore be considered. First, the floor may be stiffened to achieve a natural frequency of at least 6 Hz [8], thereby statistically reducing the risk of second-harmonic resonance, since musical beat frequencies are rarely above 3 Hz (Figure 13). Nevertheless, at 6 Hz the structure remains potentially sensitive to third-harmonic resonance, although its contribution is lower than that of the second harmonic (Figure 16). To avoid this, a target frequency of at least 8.4 Hz [5], or even 9 Hz, would be required, which is not always feasible for functional or economic reasons. For structures with natural frequencies above 6 Hz, acceleration checks may still be performed, considering that musical beats are statistically around or below 2 Hz (Figure 13). Alternatively, global damping may be increased through the use of dampers to mitigate vibration levels [1].

An additional key aspect concerns the acceleration response of the structure. At high acceleration levels, it could be assumed that occupants would be disturbed and cease loading. However, experimental observations show that synchronized jumping may continue up to at least 3–4 m/s^2 (Figure 15), contrary to panic thresholds suggested in the literature [5,7,14]. However, it is possible that this may affect coordination [25] and it remains to be studied in greater detail. Beyond 4 m/s^2, it would be valuable to determine the acceleration threshold at which the crowd can no longer sustain synchronized jumping.

The experiments show that occupants in contact with the structure can significantly reduce vibration levels through crowd–structure interaction (Table 7), resulting in an equivalent damping ratio that may largely exceed the intrinsic structural damping (Section 3.2.1). However, synchronized jumping does not appear to generate a comparable increase in damping (Table 7).

Given the reduced perception of vibration during jumping and the limited associated damping, particular caution is required when designing low-damped structures susceptible to resonance under such loading conditions.

4.3. Fatigue

Although resonance effects appear manageable in most cases, the cumulative nature of repeated events raises a critical issue: fatigue. The study highlights the wide variability of musical tempos (Figure 13) and the influence of musical composition (Figure 14) on crowd behavior, primarily bobbing and jumping (Figure 10). Fatigue assessment therefore requires a realistic representation of the load-cycle distribution expected during concerts. Excessive conservatism should be avoided: spectators do not continuously excite the structure at critical frequencies, and periods of reduced activity are common. In such phases, increased crowd–structure contact may significantly enhance damping.

Nevertheless, fatigue verification remains necessary. It should be emphasized that overly conservative assumptions may rapidly lead to highly restrictive estimates of the allowable number of events for the intended use. A 50-year sensitivity study conducted on a real steel floor subjected to second-harmonic resonance—based on SCI P354 coefficients and crowd densities of two to three persons/m^2 engaged in dancing and jumping, with already significant damping assumptions (3.6% to 5%)—has previously demonstrated this effect [1,35].

5. Conclusions

The experimental study demonstrates that the effects of crowd–structure interaction—specifically regarding impact, resonance, and fatigue—are significant and must not be neglected in structural design. However, these effects were found to be less critical than those predicted by the conservative coordination assumptions set out in BRE Digest 426.

The main contribution of this work lies in the experimental quantification of coordination levels for groups of up to 97 synchronized jumping individuals, thereby extending the existing literature. The results also underscore the substantial variability in behavior within large crowds and the significant damping introduced by individuals in contact with the structure. Human–structure interaction can thus mitigate dynamic amplification, provided that fully synchronized jumping is avoided. The equivalent damping ratio depends strongly on the number of occupants, their posture, and the type of excitation. For design purposes, additional damping provided by the crowd during synchronized jumping should be neglected, as jumping may partially decouple human–structure interaction. In contrast, for static or bobbing crowds, the simplified model proposed here offers a practical and sufficiently accurate tool for standard engineering applications. While more sophisticated stochastic models are available for advanced analysis, the proposed approach achieves a balance between accuracy and usability.

These findings emphasize the need for design approaches that integrate realistic coordination levels, human-induced damping, and probabilistic fatigue scenarios to ensure both the safety and the structural efficiency of floors intended for event use.

Author Contributions: Conceptualization, V.B.; methodology, V.B.; validation, L.A. and P.A.; formal analysis, V.B.; investigation, V.B. and L.A.; resources, V.B. and L.A.; data curation, V.B.; writing—original draft preparation, V.B.; writing—review and editing, V.B.; visualization, V.B.; supervision, P.A.; project administration, V.B. and L.A.; funding acquisition, V.B. All authors have read and agreed to the published version of the manuscript.

Funding: This research was funded by Setec bâtiment and supported by Cartier & Cie.

Data Availability Statement: Extensive data can be found at: https://hal.science/hal-04906126v1 (accessed on 23 March 2026). Reference [1] includes a more detailed description of the tests summarized in this paper, as well as the main datasets underlying the reported tables and figures. Raw data files (accelerations, velocities, and displacements recorded by each device) are available upon request. Video recordings of the experiments are not publicly available due to the consent agreement signed with the participants. All participants were assigned identification numbers to ensure data anonymization (weight, height, gender, age, and position). Photographs included in reference [1] provide sufficient context to understand the experimental setup without access to the videos.

Acknowledgments: The authors gratefully acknowledge SMB for supplying the steel structure, PETIT for the concrete works and scaffolding, TAYLOR for providing the dampers, BTP Consultant for the safety assessment, ULiège for the shaker testing, and the ENSAPVS administration and students for their participation in the experimental campaign. The experimental laboratory testing campaign was conducted under a formal agreement between Setec Bâtiment and the EMGCU laboratory.

Conflicts of Interest: The authors declare no conflicts of interest. The funders had no role in the design of the study, in the collection, analyses, or interpretation of data, in the writing of the manuscript, or in the decision to publish the results.

References

1. Baumann, V. Interaction Foule-Structure sur les Planchers à Usage Evénementiel. Crowd-Structure Interaction on Building Floors for Event Use. Ph.D. Thesis, Université Gustave Eiffel, Champs-sur-Marne, France, 2024.
2. *BS 6399*; Loading for Buildings. Part 1. Code of Practice for Dead and Imposed Loads. BSI Publications: London, UK, 1996.
3. British Standards Institution. *UK National Annex to Eurocode 1: Actions on Structures*; Part 1-1: General Actions; BSI: London, UK, 2005.
4. Ellis, B.R.; Ji, T. *Digest 426: The Response of Structures to Dynamic Crowd Loads*; BRE: Watford, UK, 2004.
5. Smith, A.L.; Hicks, S.J.; Devine, P.J. *Design of Floors for Vibration, a New Approach*; Revised Edition; SCI P354; The Steel Construction Institute: Bracknell, UK, 2009.
6. Bachmann, H.; Ammann, W. *Vibrations in Structures Induced by Man and Machines*; International Association for Bridge and Structural Engineering (IABSE): Zurich, Switzerland, 1987.

7. Bachmann, H.; Ammann, W.J.; Deischl, F.; Eisenmann, J.; Floegl, I.; Hirsch, G.H.; Klein, G.K.; Lande, G.J.; Mahrenholtz, O.; Natke, H.G.; et al. *Vibration Problems in Structure/Practical Guidelines*; Birkhaüser: Basel, Switzerland, 1997.
8. Canadian Commission on Building and Fire Codes. *Commentary D: Deflection and Vibration Criteria for Serviceability and Fatigue Limit States, in User's Guide—NBC 2005 Structural Commentaries (Part 4 of Division B)*; National Research Council of Canada: Ottawa, ON, Canada, 2006; pp. 25–34.
9. American Institute of Steel Construction. Steel Design Guide Series 11. In *Floor Vibrations Due to Human Activity*; AISC/CISC: Chicago, IL, USA, 1997.
10. Applied Technology Council. ATC Design Guide 1. In *Minimizing Floor Vibration*; ATC: Redwood City, CA, USA, 1999.
11. *NF EN 1991-1-1*; Eurocode 1—Actions sur les Structures—Partie 1-1. AFNOR: Saint-Denis, France, 2003.
12. SETRA; AFGC. *Passerelles Piétonnes—Evaluation du Comportement Vibratoire Sous L'action des Piétons*; SETRA: Bagneux, France, 2006.
13. HIVOSS. *Contrôle Vibratoire des Planchers, Document de Référence, Research Fund for Coal and Steel*; European Commission (via Research Fund for Coal and Steel, RFCS): Luxembourg, 2008.
14. *ISO 10137*; Bases for Design of Structures—Serviceability of Buildings and Walkways Against Vibrations. ISO: Geneva, Switzerland, 2007.
15. Reynolds, P.; Pavic, A. Vibration performance of a large cantilever grandstand during an international football match. *ASCE J. Perform. Constr. Facil.* **2006**, *10*, 202–212. [CrossRef]
16. Jones, C.; Reynolds, P.; Pavic, A. Vibration serviceability of stadia structures subjected to dynamic crowd loads: A literature review. *J. Sound Vib.* **2010**, *330*, 1531–1566. [CrossRef]
17. Shahabpoor, E.; Pavic, A.; Racic, V.; Zivanovic, S. Effect of group walking traffic on dynamic properties of pedestrian structures. *J. Sound Vib.* **2016**, *387*, 208–225. [CrossRef]
18. Xiong, J.; Chen, J.; Caprani, C. Spectral analysis of human-structure interaction during crowd jumping. *Appl. Math. Model.* **2021**, *89*, 610–626. [CrossRef]
19. Martinelli, L.; Racic, V.; Dal Lago, B.; Foti, F. Testing walking-induced vibration of floors using smartphones recordings. *Robotics* **2020**, *9*, 37. [CrossRef]
20. Racic, V.; Brownjohn, J.M.; Wang, S.; Elliot, M.T.; Wing, A. Effect of sensory stimuli on dynamic loading induced. In Proceedings of the 31st IMAC, A Conference on Structural Dynamics, Garden Grove, CA, USA, 11–14 February 2013; Topics in Dynamics of Civil Structures. Volume 4.
21. Racic, V.; Chen, J.; Pavic, A. Advanced Fourier-Based Model of Bouncing Loads. In *Conference Proceedings of the Society for Experimental Mechanics Series*; Springer: Cham, Switzerland, 2019.
22. Racic, V.; Pavic, A. Stochastic approach to modelling of near-periodic jumping loads. *Mech. Syst. Signal Process.* **2010**, *24*, 3037–3059. [CrossRef]
23. Ellis, B.; Ji, T. *Loads Generated by Jumping Crowds: Experimental Assessment*; BRE: Watford, UK, 2002.
24. Ellis, B.; Ji, T. Loads generated by jumping crowds: Numerical modelling. *Struct. Eng.* **2004**, *82*, 35–40.
25. Abraham, N.M.; Williams, G.; Zivanovic, S. Impact of vertical vibrations on human rhythmic jumping. *Structures* **2023**, *57*, 105154. [CrossRef]
26. Gaspar, C.; Caetano, E.; Moutinho, C.; Silva, J. Active human-structure interaction during jumping on floors. *Struct. Control. Health Monit.* **2019**, *27*, e2466. [CrossRef]
27. Czwikla, B.; Kasperski, M. Damping Induced by bobbing or jumping persons. In Proceedings of the X International Conference on Structural Synamics, EURODYN 2017, Rome, Italy, 10–13 September 2017.
28. McDonald, M.; Zivanovic, S. Measuring Ground Reaction Force and Quantifying Variability in Jumping and Bobbing Actions. *J. Struct. Eng.* **2017**, *143*, 04016161. [CrossRef]
29. The Institution of Structural Engineers. *Dynamic Performance Requirements for Permanent Grandstands Subject to Crowd Action: Recommendations for Management, Design and Assessment*; The Institution of Structural Engineers: London, UK, 2008.
30. Parkhouse, J.; Ewins, D. Crowd-induced rhythmic loading. *Struct. Build.* **2006**, *159*, 247–259. [CrossRef]
31. Hashim, R.; Ji, T.; Mandal, P.; Zhang, Q.; Zhou, D. Human-structure interaction experiments to determine the dynamic properties of the standing human body in vertical vibration. *Structures* **2020**, *26*, 934–946. [CrossRef]
32. Matsumoto, Y.; Griffin, M. Mathematical models for the apparent masses of standing subjects exposed to vertical whole-body vibration. *J. Sound Vib.* **2003**, *260*, 431–451. [CrossRef]
33. Allani, A. Conception et Optimisation D'amortisseurs à Masse Accordée Pour les Structures du Génie Civil. Ph.D. Thesis, Université Paris-Est, Champs-sur-Marne, France, Università Degli Studi di Roma "Tor Vergata", Rome, Italy, 2015.

34. *NF EN 1993-1-1/NA*; Eurocode 3—Calcul des Structures en Acier—Partie 1-1: Règles Générales et Règles Pour les Bâtiments—Annexe Nationale. AFNOR: Saint-Denis, France, 2013.
35. Baumann, V.; Botero, M. Vérification à la fatigue des planchers à usage événementiel. *Rev. Constr. Métallique CTICM* **2022**, *2*, 71–114.